A GRAPHICAL METHOD FOR DETERMINING TRUSS STABILITY

Cameron MILLAR*, Allan McROBIE, William F. BAKER[a]

*University of Cambridge. Department of Engineering, Trumpington Street, Cambridge, CB2 1PZ, cgm37@cam.ac.uk
[a]Skidmore, Owings & Merrill

Editor's Note: The first author of this paper is one of the five winners of the 2020 Hangai Prize, awarded for outstanding papers that are submitted for presentation and publication at the annual IASS Symposium by younger members of the Association (under 30 years old). It is published here with permission of the editors of the proceedings of the IASS Symposium 2020/21 "Inspiring the Next Generation", that will be held in August 2021 in Guildford, UK.

DOI: Digital Object Identifier to be provided by Editor when assigned upon publication

ABSTRACT

Graphic statics has been used for over 150 years, having been pioneered by the likes of Maxwell, Cremona, Culmann and Rankine, and has recently seen a resurgence in popularity because of its use in design. However, it is only concerned with equilibrium; as any engineer will testify, whilst equilibrium is necessary, it is not sufficient and stability must also be obtained. This paper develops a novel graphical method for determining the stability and stiffness of prestressable structures. By considering the weighted sum of the Maxwell-Minkowski diagram, the stiffness and stability of the structural mechanisms can be determined. This work extends to cover structures with multiple mechanisms and has been compared to results obtained through experimentation and the finite element method. Furthermore, it extends the work on stiffness to provide a graphical method to estimate the natural frequency of a truss. Whilst this method accurately determines the stiffness of structures, it represents a significant development in the field of graphic statics as it allows an engineer to 'eye-ball' the stability of a given truss. Engineers can also manipulate the form and force diagrams, as desired, to adjust the stiffness of their structure accordingly, whilst being able to visualise the process. Much of the previous work in this area relies heavily upon large matrices, while this method allows a more intimate and hands-on alternative.

Keywords: *Graphic Statics, Design, Stability, Tensegrity, Mechanisms, Dual Structures, Self-stress, Reciprocal Diagrams, Maxwell.*

1. INTRODUCTION

Graphic statics has been used to evaluate the relationship between form and force since the 19th century [1]. It evaluates structural equilibrium through two dual diagrams; one representing the geometry of a pin jointed truss and the other showing the equilibrium of forces. These reciprocal diagrams can be found through different methods (Cremona and Rankine) which are generally well understood [1]. These methods are very powerful in design and can be used to optimize structures [2]. One consequence of optimization is that diagonal bracing members are often removed as they carry no load in an equilibrium analysis of the structure (for the load case which was used to optimize the structure). However, they provide stiffness, stability and redundancy. Engineers, such as Robert Maillart, used these principles to design highly efficient and elegant structures such as the Chiasso Shed, which is discussed in Section 6. However, the quads within these structures imply the presence of mechanisms. These structures often rely on the stiffness of the connections (graphic statics assumes the trusses are pin-jointed) to produce stiff structures. However, it is still important to develop new ways to consider the stability of such structures. Another area of interest is that of tensegrities. Previous work by Guest [3], Connelly [4] and Pellegrino [5] have previously considered prestress rigidity and stability but rely upon the computation of large matrices and so give many engineers little insight into the structural behaviour. Therefore, these methods are used primarily to analyse structures whereas this new method aims to empower the designer and assist in structural design problems.

2. PRESTRESS STABILITY

This theory relies upon a few simple and common assumptions. Firstly, we will only consider pin-jointed trusses, as is common throughout graphic statics. This simplification is found throughout structural engineering and is a good approximation

for many structures, including tensegrities, which are considered in this paper. Furthermore, we will assume that all members are inextensionable. This is because the mechanisms are typically far less stiff than the extensionable modes of the structure. Therefore, the majority of the deflections will come from the mechanism and so it is reasonable to discard the extensionable effects. Furthermore, the strains in truss members are typically small.

We shall consider the work done when the structure undergoes a small perturbation about its equilibrium position. The internal work done, *WD*, by a nodal displacement, $\boldsymbol{d}$,is given as

$$WD = \frac{1}{2}\boldsymbol{d}^{\boldsymbol{T}}\boldsymbol{K}\boldsymbol{d} \tag{1}$$

It can also be shown that the tangent stiffness matrix, $\boldsymbol{K}$, is given by [3]

$$\boldsymbol{K} = \boldsymbol{A}\widehat{\boldsymbol{G}}\boldsymbol{A}^T + \boldsymbol{S} \tag{2}$$

where $\boldsymbol{A}$ is the equilibrium matrix, $\widehat{\boldsymbol{G}}$ is a diagonal matrix of modified axial stiffnesses and $\boldsymbol{S}$ is the stress matrix (note that $\boldsymbol{S}$ has units of N/m and not N/m^2 as it comes from the mathematical field of rigidity theory rather than engineering [4]).

We will restrict our attention to the analysis of mechanisms. This is because of the assumption of inextensionable members. These lie in the left-null-space of $\boldsymbol{A}$ so that $\boldsymbol{A}^T\boldsymbol{m} = \boldsymbol{0}$ [5]. Therefore, the work done by a mechanism is

$$WD = \frac{1}{2}\boldsymbol{m}^T\boldsymbol{S}\boldsymbol{m} \tag{3}$$

We can also define a generalised stiffness $K_s = \overline{\boldsymbol{m}}^T\boldsymbol{S}\overline{\boldsymbol{m}}$ where $\overline{\boldsymbol{m}} = \frac{\boldsymbol{m}}{|\boldsymbol{m}|}$ is a unit vector. If $K_s > 0$ then the structure is stable, if $K_s < 0$ then it is unstable and if $K_s = 0$ then it is neutrally stable. Typically, an engineer wants a structure to be stiff, but sometimes neutral stability (such as in an Anglepoise lamp) or negative stiffness is desirable such as in seismic damper applications.

The stress matrix, $\boldsymbol{S}$, is defined as [3]

$$\boldsymbol{S} = \begin{pmatrix} \boldsymbol{S}_{p_{11}} & \cdots & \boldsymbol{S}_{p_{1n}} \\ \vdots & \ddots & \vdots \\ \boldsymbol{S}_{p_{n1}} & \cdots & \boldsymbol{S}_{p_{nn}} \end{pmatrix} \tag{4}$$

where for $i = j$,

$$\boldsymbol{S}_{p_{ii}} = \hat{t}_{ii}\boldsymbol{I} \tag{5}$$

and $\hat{t}_{ii}$ is the sum of the force densities which meet at node i. $\boldsymbol{I}$ is the identity matrix, 2×2 for 2D trusses and 3×3 for 3D trusses. For $i \neq j$

$$\boldsymbol{S}_{p_{ij}} = \hat{t}_{ij}\boldsymbol{I} \tag{6}$$

where $\hat{t}_{ij}$ is the force density in the bar connecting node i to node j (tension is positive and $\hat{t}_{ij} = 0$ if the nodes are not connected). A force density is defined as $\hat{t} = {}^{T}/_{L}$ for each bar. This can be proved in numerous other ways; one to note is that of Connelly who uses a minimum energy function to determine the stress matrix (second-order rigidity) [4]. In graphic statics, we can determine L from the form diagram and T from the force diagram.

This formulation can be expanded into a sum over all the bars

$$WD = \frac{1}{2}\sum_{bars}\frac{T}{L}(\boldsymbol{b}-\boldsymbol{a})\cdot(\boldsymbol{b}-\boldsymbol{a}) \tag{7}$$

where $\boldsymbol{b}$ and $\boldsymbol{a}$ are the deflections of each end of the bar. The ${}^{T}/_{L}$ term is the force density in the bar and is the aspect ratio of the rectangle in the 2D Maxwell-Minkowski diagram [6]. However, its interpretation

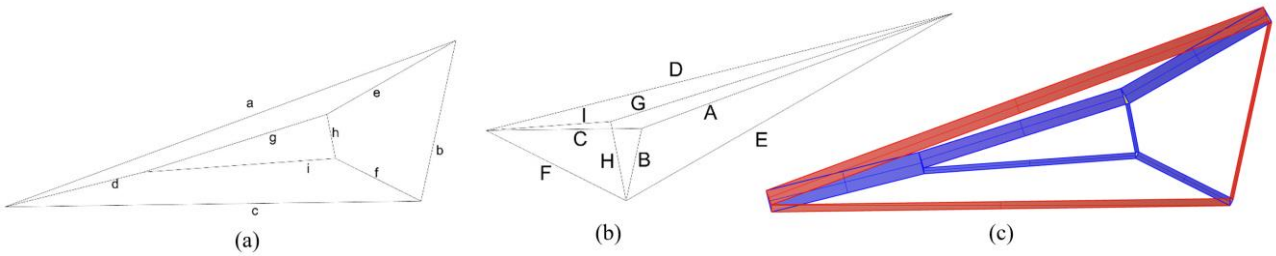

Figure 1: *Maxwell Fig IV [11]. (a) From diagram. (b) Force diagram which is reciprocal (Cremona construction). (c) Maxwell-Minkowski diagram [6].*

in 3D is less obvious. Therefore, (7) is reworked into (8).

$$WD = \frac{1}{2}\sum_{bars} TL\Phi^2 \qquad (8)$$

where $\Phi = \frac{|\boldsymbol{b}-\boldsymbol{a}|}{L}$ and is a weight function. Φ is also the rotation of the bar in the mechanism. This method immediately generalises to 3D (in both Rankine and Cremona construction) and to out-of-plane mechanisms. We can consider TL to be the 'rotational stiffness' of the bar. A Maxwell-Minkowski diagram is constructed from a summation of the form and force diagram [6], as shown in Figure 1. In 3D, we use a Rankine-Minkowski diagram [6], but here we will use the two interchangeably. The TL term is the area of the rectangle corresponding to the bar in 2D and the volume of the cuboid in 3D. This is a more physical interpretation of the formulation than the matrix methods previously used. For example, the Jessen Icosahedral tensegrity has a mechanism in which none of the struts (compression members) rotate. Therefore, this must be stable as there is no negative contribution to the stiffness. A fuller description of this method is given in McRobie *et al* [12].

2.1. Mechanisms

It is desired that the stability of the truss can be determined entirely through graphical methods. It is possible to find the m independent internal mechanisms of a structure through at least two different graphical methods. One is more suited for a planar system; here, the Airy stress function over the dual diagram (force) can be used [8]. The plane-faced polyhedron (Airy stress function) requires $3 + 1 + m$ points to be defined (the 1 here refers to a rigid body rotation). By increasing the height of a node slightly while maintaining planarity of faces, the change to the form diagram is found. Rotating the change by 90° gives the mechanism of the structure. Another method involves the sliding of blocks past each other [9]. For 3D structures, the second method is more suitable as the Airy stress function is harder to visualise (it is in 4D). It is possible to confirm that any mechanism does not violate the constraint of inextensionable members by ensuring that $(\boldsymbol{b}-\boldsymbol{a})\cdot\boldsymbol{l}=\boldsymbol{0}$ for all bars, where $\boldsymbol{l}$ is a vector aligned with the bar.

2.2. Deflections

We have the work done by activating the mechanism in the form of $\mathrm{WD} = \frac{1}{2}\mathrm{K_s}\delta^2$ where $\delta = |\boldsymbol{m}|$. Therefore, we have the stiffness, K_s, which corresponds to a deflection δ. It is important that K_s is defined with respect to δ as δ could be a rotation (giving K_s as a rotational stiffness), a deflection in the direction of the mechanism, or in a different associated direction. From this, it is possible to calculate the force, F_δ, acting in the same direction as $\boldsymbol{m} = \delta\bar{\boldsymbol{m}}$, and therefore calculate the deflection, $\delta = {}^{F_\delta}/_{K_s}$. This stiffness is proportional to the prestress in the structure (from (8)). Therefore, it is possible to calculate the prestress required to limit the deflection. An exemplar case is that of a 2D tensegrity dome, as shown in Figure 2.

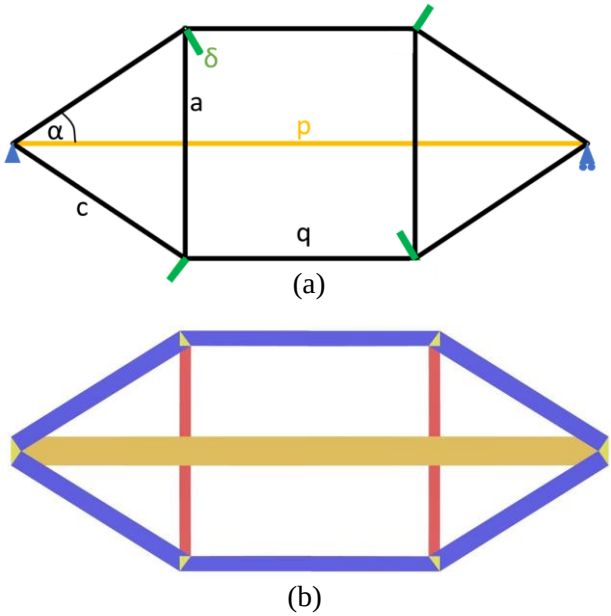

Figure 2: *Tensegrity Dome. (a) From diagram and the associated mechanism. (b) Maxwell-Minkowski diagram.*

The mechanism is far less stiff than the extensional motions (so our assumption of inextensionable bars is valid). We can find the internal work done by the mechanism;

$$\begin{aligned} WD &= \frac{1}{2}\sum_{bars} TL\Phi^2 \\ &= \frac{1}{2}\left\{4T_cL_c\left(\frac{\delta}{L_c}\right)^2 \right. \\ &\quad + 2T_qL_q\left(\frac{2\delta\cos\alpha}{L_q}\right)^2 \\ &\quad \left. + 2T_aL_a\left(\frac{2\delta\ \sin\alpha}{L_a}\right)^2\right\} \end{aligned} \qquad (9)$$

This can be simplified using the Maxwell Load path theorem $\sum_{bars} TL = 0$ [6] (in the absence of external loads) and through geometry to give

$$WD = \frac{1}{2}\left\{-\frac{2T_p L_p \cos\alpha}{L_q L_c}\right\}\delta^2 = \frac{1}{2}K_s\delta^2 \quad (10)$$

Clearly the dome is stable for bar p in compression, as expected. Applying a vertical downward point load to the node connecting *c* and *q*, we can calculate the deflections of this node. The work done by this external load is

$$WD = F\delta\cos\alpha = F_\delta\delta \quad (11)$$

Using the stiffness associated with a deflection δ, we can find the deflection of the truss

$$\delta = \frac{F_\delta}{K_s} = \frac{F\cos\alpha}{\left(-\frac{2T_p L_p \cos\alpha}{L_q L_c}\right)} \quad (12)$$

A similar method can be used to find the deflections of more complicated frameworks. The deflections can also be found by equating the internal and external work – setting (10) equal to (11).

2.3. Subtleties of the theory

The theory presented works well for many cases, but there are some exceptions where care must be taken. The stiffness discussed comes from geometric changes in the structure. This can be shown from the example of the pendulum; there are no bar extensions but it is the change in the line of forces which produces stiffness. Therefore, this analysis is valid in both the elastic and plastic regimes as the axial forces can still be found through graphic statics. The Maxwell-Minkowski diagram actually is the perfect lower bound solution to the problem as it gives the exact dimensions of every member of the structure so that every member yields at the same prestress.

2.3.1 Rigidity and Finite Mechanisms

So far, we have investigated prestress stable structures. These are often tensegrities. The structures are only stiff because of their prestress. Connelly's derivation of the stiffness matrix considers only second-order bar extensions (no first-order extensions as this would violate the requirements of a mechanism) experienced when the mechanism is activated. All prestress stable structures are second-order rigid [4]. It can be shown that second-order rigidity implies stability of the structure [4].

This method is valid for the evaluation of any mechanism. A finite mechanism allows nodes to move freely for a finite distance. An infinitesimal mechanism allows nodes to move with no first-order changes in member length (higher-order length changes do occur). Finite mechanisms cannot be stabilised and $K_s = 0$ (neutral stability) [9]. Rigid body rotations are also neutrally stable as every bar rotates by the same amount, Φ. Therefore, $K_s = \Phi^2 \sum_{bars} TL$. The Maxwell Load path theorem states that $\sum_{bars} TL = 0$ [6] meaning that $K_s = 0$. An example of an internal finite mechanism is that of the Steffen polyhedron which is the simplest non-crossing flexible polyhedron and is based on the Bricard octahedron. Applying the method developed here to this problem gives $K_s = 0$, as expected.

If this analysis gives $K_s = 0$ for a structure, then it is considered to be neutrally stable in the second-order sense. However, there may be third or higher-order bar extensions which were not considered which may result in the structure being either stable or unstable [5]. However, it is likely that these higher-order changes in member lengths will result in a small change in stiffness so that $K_s \approx 0$ meaning the assumptions made here are reasonable. Neutral stability of infinitesimal mechanisms is a purely mathematical concept which cannot be achieved in practice as it will be either stable or unstable [9].

2.3.2 Multiple Mechanisms

Some structures have multiple mechanisms associated with them. It is important to be able to determine which mechanism has the smallest stiffness associated with it. To do this, first we define a mechanism space, $\boldsymbol{M}$, so that any mechanism $\boldsymbol{v} = \alpha\boldsymbol{m}_1 + \beta\boldsymbol{m}_2$ ... can be found through $\boldsymbol{v} = \boldsymbol{M}\boldsymbol{h}$. All the basis mechanisms, $\boldsymbol{m}_1, \boldsymbol{m}_2$ ..., are orthonormal (can be found through Gram-Schmidt orthogonalization). A correction for non-orthonormal basis mechanisms can be made and is discussed in greater depth in other papers by the authors [13].

$$\boldsymbol{M} = \begin{pmatrix} \vdots & \vdots \\ \boldsymbol{m}_1 & \boldsymbol{m}_2 \\ \vdots & \vdots \end{pmatrix} \quad (13a)$$

$$\boldsymbol{h} = \begin{pmatrix} \alpha \\ \beta \\ \vdots \end{pmatrix} \tag{13b}$$

We want to determine the minimum value of K_s so we find

$$min(K_s) = min(\boldsymbol{v}^T \boldsymbol{S} \boldsymbol{v}) \tag{14}$$

$$min(K_s) = min(\boldsymbol{h}^T (\boldsymbol{M}^T \boldsymbol{S} \boldsymbol{M}) \boldsymbol{h}) \tag{15}$$

If we have m mechanisms, we can then obtain a $m \times m$ matrix $\bar{\boldsymbol{K}} = \boldsymbol{M}^T \boldsymbol{S} \boldsymbol{M}$. Here, $\bar{\boldsymbol{K}}$ is the same as the reduced stress matrix, $\boldsymbol{Q}$, derived by Pellegrino [5][3]. The eigenvectors of $\bar{\boldsymbol{K}}$ give the values of α and β corresponding to the stiffest and least stiff mechanisms. It is possible to find $\bar{\boldsymbol{K}}$ through graphical methods as

$$\bar{\boldsymbol{K}} = \begin{pmatrix} \boldsymbol{m}_1{}^T \boldsymbol{S} \boldsymbol{m}_1 & \boldsymbol{m}_1{}^T \boldsymbol{S} \boldsymbol{m}_2 & \cdots \\ \boldsymbol{m}_2{}^T \boldsymbol{S} \boldsymbol{m}_1 & \boldsymbol{m}_2{}^T \boldsymbol{S} \boldsymbol{m}_2 & \\ \vdots & & \ddots \end{pmatrix} \tag{16}$$

$\bar{\boldsymbol{K}}$ is a real symmetric matrix as $\boldsymbol{m}_i{}^T \boldsymbol{S} \boldsymbol{m}_j = \boldsymbol{m}_j{}^T \boldsymbol{S} \boldsymbol{m}_i$. The components of $\bar{\boldsymbol{K}}$ can be found using the following weighted sum of the Maxwell-Minkoswki diagram.

$$\boldsymbol{m}_i{}^T \boldsymbol{S} \boldsymbol{m}_j = \sum_{bars} T\, L \Phi_i \cdot \Phi_j \tag{17}$$

where Φ_i is the rotation of the bar in mechanism i. Note that we take the dot product of the two rotations; this is easy to do for planar trusses as all rotations are aligned with the **k** vector. However, in 3D, care must be taken here.

If all the eigenvalues of $\bar{\boldsymbol{K}}$ are positive, then the structure is stable. Another way of viewing this is if $\bar{\boldsymbol{K}}$ is positive definite, then the structure is stable. This can be checked using Sylvester's criterion. If $\bar{\boldsymbol{K}}$ is negative definite, then a reversal of the prestress will result in a positive definite case. This is the case for structures with only one mechanism; a reversal of prestress will convert an unstable structure into a stable one. If a structure has both positive and negative eigenvalues, a reversal of stresses will not stabilise the structure. Furthermore, if there are positive and negative eigenvalues, there will also exist a mechanism with neutral stability. This can be found by calculating the null-space (or left-null-space as $\bar{\boldsymbol{K}}$ is symmetric) of $\bar{\boldsymbol{K}}$. This will give $K_s = \boldsymbol{h}^T \bar{\boldsymbol{K}} \boldsymbol{h} = 0$ by definition and can be a useful check on whether a rigid body rotation has been included in the mechanism space. The zero stiffness mechanism is not necessarily a eigenvector of $\bar{\boldsymbol{K}}$. For many structures, the number of mechanisms is small so it is possible to consider $\bar{\boldsymbol{K}}$ by hand.

An example of how this can be done is Maxwell Fig V [11], as shown in Figure 3. This truss has one state of self-stress and two mechanisms. The question is, which mechanism is the least stiff? The mechanisms can be found through the Airy stress function approach [8] discussed in Section 2.1 and then $\bar{\boldsymbol{K}}$ can be determined.

$$\bar{\boldsymbol{K}} = \begin{pmatrix} 0.0662 & 0.0037 \\ 0.0037 & 0.1610 \end{pmatrix} \tag{18}$$

$\bar{\boldsymbol{K}}$ has only positive eigenvalues so the structure is stable. The eigenvectors of $\bar{\boldsymbol{K}}$ also give the values of α and β which give the mechanism with the smallest and greatest stiffness. Here, $\mathbf{m}_a$ is the stiffest and $\mathbf{m}_b$

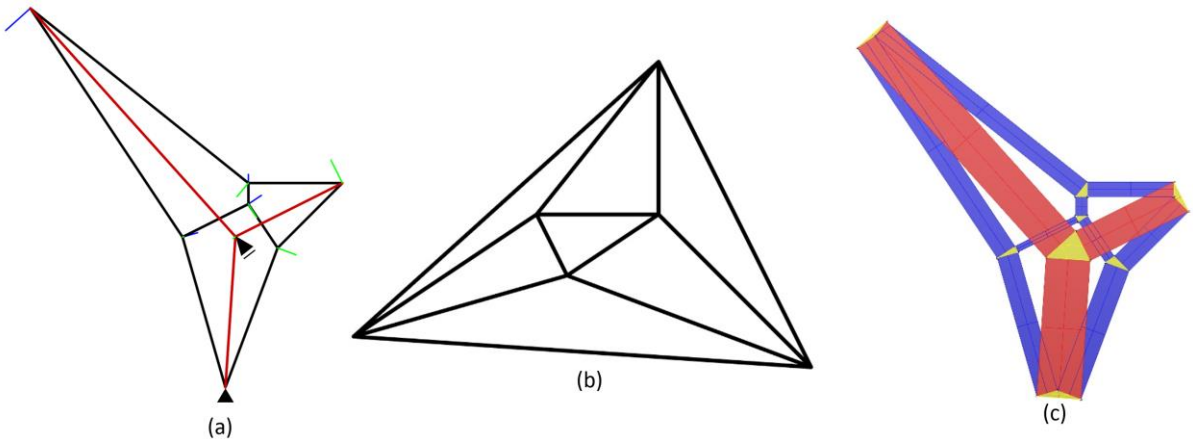

Figure 3: *Maxwell Fig V [11]. (a) Form diagram with struts in red and cables in black. $\boldsymbol{m}_1$ is shown in blue and $\boldsymbol{m}_2$ in green. (b) Force diagram. (c) Maxwell-Minkowski diagram.*

is the least stiff. They are shown in Figure 4.

$\lambda_a = 0.1612$	$\boldsymbol{m}_a = 0.0386\boldsymbol{m}_1 + 0.9993\boldsymbol{m}_2$
$\lambda_b = 0.0660$	$\boldsymbol{m}_b = 0.9993\boldsymbol{m}_1 - 0.0386\boldsymbol{m}_2$

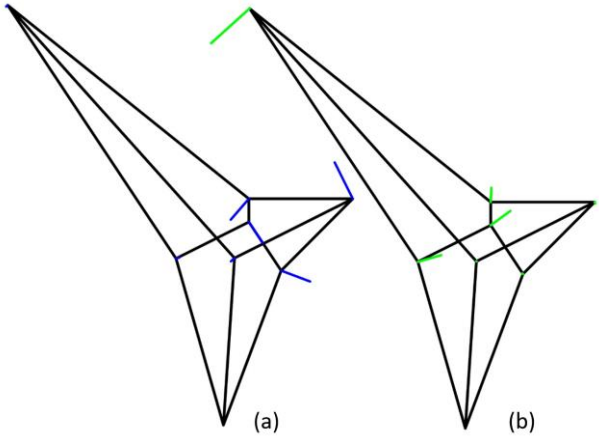

Figure 4: *Eigenvectors of Maxwell Fig V. (a) Mechanism $\boldsymbol{m}_a$. (b) Mechanism $\boldsymbol{m}_b$.*

2.3.3 Large Loads and Large Deflections

The derivations for this theory rely upon small deflections. Furthermore, the tensions in the members are assumed to be equal to that of the prestress. However, if a load is applied with a component in the column space of $\boldsymbol{A}$ (non-mechanism load path) then the axial loads could vary. Any applied load can be decomposed into an extensional component (in the column space of $\boldsymbol{A}$) and an inextensional component (in the left-null-space of $\boldsymbol{A}$) which are orthogonal [5]. Therefore, if a load is applied which lies only partially in the mechanism space, the true axial forces should be used; these can often be found through the addition of a funicular. The funicular can remove the mechanism from the structure so the axial loads should be calculated with the funicular and the mechanism without it. It is important to check that member requirements are still met, such as cables in tension and struts in compression. For small loads, the change in axial loads is negligible and the prestress forces can be used. If we apply a funicular which loads the structure partially in the mechanism space, it will not be possible to load the funicular. This is because the structure, in its current geometry, cannot find an equilibrium solution for any load in the mechanism space. Therefore, the funicular must be applied in the column-space of $\boldsymbol{A}$.

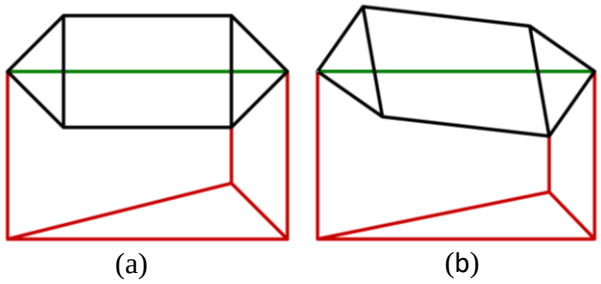

Figure 5: *Funiculars, in red, applied to a tensegrity dome (as in Figure 2). The green strut applies a constant compressive force and gets shorter as the outer triangles rotate. (a) Funicular has a component in the mechanism space so cannot be stressed. (b) Outer triangles rotate so a form and reciprocal force diagram can be constructed.*

It is possible to find the solution to large displacement problems using conventional graphic statics. Ultimately, we are trying to find an equilibrium solution to the problem, which is the primary use of graphic statics and statics in general. The funicular applied in Figure 5(a) corresponds to an external vertical load vector which is in the mechanism space of the structure, and thus the only equilibrium solution is a state of self-stress confined to the structure (and the horizontal green bar), with zero vertical loads applied. However, once the two outer triangles start to rotate, the structure is no longer a projection of a plane faced polyhedron and cannot be self-stressed. Furthermore, the funicular no longer lies in the mechanism space so it can be stressed. The Maxwell-Calladine count of this structure, including the green bar, is zero. Therefore, if it is prestressable we have a mechanism and if it is not, there is no mechanism. As the structure deflects, it loses both its state of self-stress and its mechanism. The Maxwell-Calladine count of the structure and the funicular is also zero, but in the deformed configuration it contains one mechanism (the funicular swinging) and one state of self-stress, which involves all the members, including the funicular. As there is only one state of self-stress and we know the force in the green bar, we can find the applied vertical load.

Members lengths are kept fixed, and the structure is incremented through a set of large-deformation configurations. Note in particular that the horizontal green line of action of the applied prestress shortens as the end triangles rotate, and the underlying funicular is redrawn at each configuration to ensure verticality of the applied loads and support reactions.

We fix the prestress force in this green bar. At each configuration, the vertical force which is necessary to maintain equilibrium may be calculated. The downward deflection of the loading point is readily calculated from the configuration geometry, allowing the full large displacement load-deflection curve to be found, as in Figure 6. The gradient at zero applied load gives the stiffness found in Section 2.2 and equation (10).

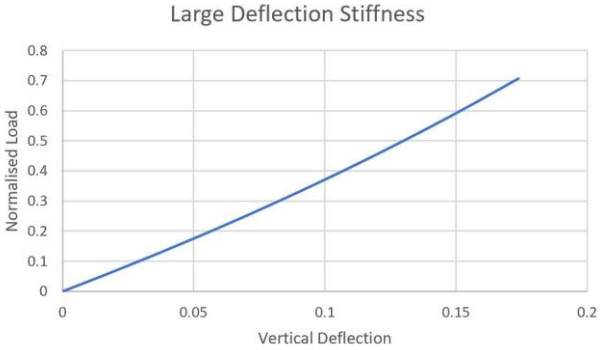

Figure 6: *Load displacement graph for a tensegrity dome. The applied load is normalised against the force in the green bar. The structure stiffness as it deflects.*

2.3.4 Vibrations

Vibrations of structures can be determined by considering the eigenstructure of $\boldsymbol{M}^{-1}\boldsymbol{K}$. However, we can use Rayleigh's principle to estimate the natural frequency of the structure for small oscillations about the equilibrium position. The problem can be simplified to that of a mass on a spring by estimating a mode shape $\boldsymbol{u}$. It is assumed that $\boldsymbol{u}$ (unit vector) is a mechanism of the structure so the stiffness can be calculated using the weighted sum of the Maxwell-Minkowski diagram $K_{eq} = K_s = \boldsymbol{u}^T\boldsymbol{S}\boldsymbol{u}$. The equivalent mass can also be determined; $M_{eq} = \boldsymbol{u}^T\boldsymbol{M}\boldsymbol{u} = \sum_i M_i {u_i}^2$.Therefore, an estimate of the natural frequency can be obtained as $\omega = \sqrt{\frac{K_{eq}}{M_{eq}}}$.

This is clearly easy to do if there is only one mechanism. For cases with multiple mechanisms, a good estimate for the natural frequency can usually be obtained by using the mode shape with the least stiffness associated with it. This can be found through the method described in Section 2.3.2.

An easy example of this method is that of a pendulum. Let us consider a light rod of length l with a mass m at the end. Traditional structural methods give the stiffness of the pendulum in a direction perpendicular to the rod as zero. Therefore, as $\omega = \sqrt{K/M}$, we determine that $\omega = 0$, which is clearly incorrect. Using this new method, we can find the stiffness associated with a small horizontal deflection, δ, as shown in (19). From this, we can then obtain the natural frequency, $\omega = \sqrt{g/l}$, as expected.

$$WD = \frac{1}{2}mgl\left(\frac{\delta}{l}\right)^2 = \frac{1}{2}\frac{mg}{l}\delta^2 = \frac{1}{2}K_s\delta^2 \tag{19}$$

$$\omega = \sqrt{\frac{K_{eq}}{M_{eq}}} = \sqrt{\frac{mg/l}{m}} = \sqrt{\frac{g}{l}} \tag{20}$$

In the special case where $\boldsymbol{M} = \rho\boldsymbol{I}$, the exact solution can be found as $\boldsymbol{M}^{-1}\boldsymbol{K} = {}^{1}/_{\rho}\,\boldsymbol{S}$. Therefore, we only care about the eigenvectors of $\boldsymbol{S}$ (considering only the mechanism space) which we can find using the method described in Section 2.3.2. In the case of the tensegrity dome ($m = 1$) considered in Section 2.2, we observe that $\boldsymbol{M} = \rho\boldsymbol{I}$ through symmetry. The mass is lumped at the nodes so that each node has a mass of ρ. We have already determined the stiffness in Section 2.2 so

$$\omega = \sqrt{\frac{K_{eq}}{M_{eq}}} = \sqrt{\frac{\left(\frac{2T_4L_4s}{q \times c^2}\right)}{\rho}} \tag{21}$$

2.3.4 Boundary Conditions

Often, the boundary conditions of a problem can be easily changed by applying a rigid body rotation. A rigid body rotation has neutral stability so it is easy to convert one problem into another by applying this. An example of this in practice is Maxwell Fig IV [11], as shown in Figure 1 and Figure 7.

Let us consider the case where all triangles are equilateral, as in Figure 7 (outside length L_3 and inner length L_1). We can find the stiffness when the outer triangle is held stationary (22) before applying a rigid body rotation ($\theta = \frac{-\delta\sqrt{3}}{L_1}$) to the summation to hold the inner triangle stationary (23).

$$WD_{outer} = \frac{1}{2}\left[3T_1L_1\left(\frac{\delta\sqrt{3}}{L_1}\right)^2 + 3T_2L_2\left(\frac{\delta}{L_2}\right)^2\right] \quad (22)$$

$$WD_{inner} = \frac{1}{2}\left[3T_1L_1\left(\frac{\delta\sqrt{3}}{L_1} - \frac{\delta\sqrt{3}}{L_1}\right)^2 + 3T_2L_2\left(\frac{\delta}{L_2} - \frac{\delta\sqrt{3}}{L_1}\right)^2 + 3T_3L_3\left(-\frac{\delta\sqrt{3}}{L_1}\right)^2\right] \quad (23)$$

$$WD_{inner} = \frac{1}{2}\left[3T_2L_2\left(\frac{\delta L_3}{L_1L_2}\right)^2 + 3T_3L_3\left(\frac{\delta\sqrt{3}}{L_1}\right)^2\right] \quad (24)$$

$$WD_{inner} = \frac{1}{2}\left[3T_2\left(\delta\frac{L_3}{L_1}\right)^2\left(\frac{1}{L_2} - \sqrt{3}\frac{1}{L_3}\right)\right] \quad (25)$$

Note that (25) is the equation you would obtain if you were to calculate it using the direct approach.

This is a classic example of a simple spider-web; the outside triangle is in compression with an inner tension triangle. Examining this example with the inner triangle fixed, we can see that it is stable for $L_2\sqrt{3} < L_3$. This is expected as it is similar to the clothes prop problem; as soon as the inner triangle inverts, the structure becomes unstable.

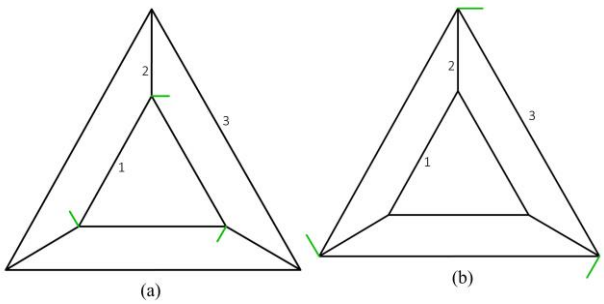

Figure 7: *Mechanisms in Maxwell Fig IV [11] (equilateral configuration). (a) Outer triangle held rigid with nodal deflection of magnitude δ. (b) Inner triangle held rigid with a nodal deflection of magnitude $\frac{L_3}{L_1}\delta$.*

3. EXPERIMENTS

The work done here develops well established theories. However, some small-scale experiments on a tensegrity dome, which has been discussed in Section 2.2, were performed. A prestress was applied and then incremental vertical loads were applied to the node, as shown in Figure 8. The vertical displacement of the node was then measured using a laser. The laser was used as any contact with the node would have a large impact on the results as it would provide a force on the structure which has very little stiffness in that direction. The deflection was then plotted against the applied load and the stiffness calculated. The stiffness was proportional to the prestress applied, as expected. Therefore, if we divide the stiffness by the prestress, we obtain a number which is function of the geometry only.

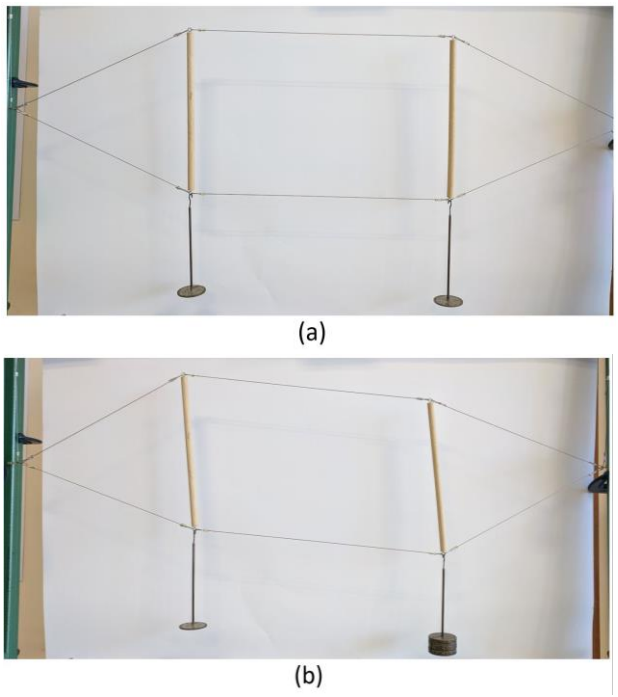

Figure 8: *Experimental set up for a tensegrity dome. (a) Unloaded. (b) Loaded.*

The full experimental results are not published here. However, the method is detailed here. For a tensegrity dome, as in Figure 2, with a geometry of $l_a = 217mm$, $l_q = 347mm$ and $l_p = 807mm$, we can obtain the graph shown in Figure 9(a).

The experiments showed good correlation with the theory, as shown in Figure 9(b). Some discrepancies were seen when the rotations were large; the experimental stiffness was greater than that predicted using the theory developed here (note the

large displacement method discussed in Section 2.3.3 was not used). The mechanism is infinitesimal so the structure will stiffen as it deflects, as discussed in Section 2.3.3.

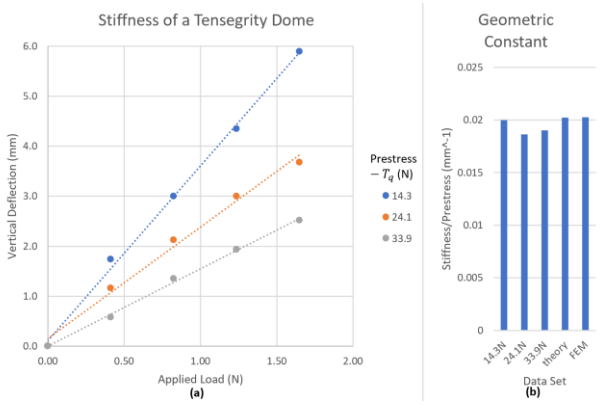

Figure 9: *Stiffness of a Tensegrity Dome for varying prestress.*

Further experiments on different configurations were performed and the theory correctly predicts which structures are unstable and the stiffness of stable structures. For some structures, the stiffness is very sensitive to the geometry. It was noted that structures which had a very small positive stiffness underwent large deflections. Therefore, when designing structures such as tensegrities, it is important to check that the structure is not only stable but also does not undergo large deflections (confirm the assumptions in Section 2 are valid). If it does undergo large deflections, it is possible to increase the stiffness by increasing the prestress in the structure for the same geometry or by modifying the structural geometry.

4. THE FINITE ELEMENT METHOD (FEM)

Strand7 was used as a comparison to experimental results. The FEM uses a non-linear geometry solver to calculate the deflections but provides little insight into the behaviour of structures, unlike the method described in this paper. The structure can carry applied loads through a combination of changes in geometry and changes in member forces [5]. The method developed here only considers changes in geometry as the members are inextensionable, whilst FEM considers the contribution of both effects.

The results from the FEM analysis of a tensegrity dome agree very closely with those found through our method and, therefore, also with experimental data, as shown in Figure 9b. The truss members were modelled as having a large axial stiffness, EA, so that the member strains were very small. Furthermore, it predicted unstable structures well; they were recognisable as when the load was removed the structure did not return to its undeformed configuration.

5. DESIGN VERSUS ANALYSIS

The methods developed here are useful for designers. It informs the engineer as to which members contribute most to the stiffness of the structure. Unlike FEM, it informs the designer and provides insight into the behaviour of the structure. FEM is good for the analysis of structures but is less applicable for design work. These graphical methods can be easily integrated into software which gives excellent results if the assumptions made are reasonable (which they often are).

This method allows the engineer to ‘eye-ball’ the stability of the structure by considering the weighted sum of the Maxwell-Minkowski diagram. For example, Maxwell Fig V [11] (discussed in Section 2.3.2 and shown in Figure 3) we expect to be stable. This is because the weighted sum of the Maxwell-Minkowski diagram for the compression members and the outer cables are approximately equal. We can see this as at each outer node, the compression force is approximately twice the tension force in each cable. The lengths are approximately equal, as are the rotations. As these members approximately cancel and as the only other members are tension members, we expect the structure to be stable. It is easier to ‘eye-ball’ the stability when we only consider one mechanism.

One type of structure which is often designed using graphical methods is cable nets. SOM have collaborated with Janet Echelman to install numerous art installations using cable nets designed using graphic statics. A recent project at Princeton University has dancers on the cable net. It is desired that there is only one state of self-stress so that the forces in each cable can be known accurately. There are also multiple mechanisms in the cable net so that dancers can morph the net. Using FEM, it is not possible to identify which mechanism is the least stiff, only the deflections of the cable net under a given load. Furthermore, it does not show how each member contributes to the stiffness of the structure. This method allows the designer to find the critical mechanism and allows for a more intuitive method for adjusting the geometry of the problem so as to

achieve the desired outcome.

6. CHIASSO SHED

Graphic statics has been used in the design and optimisation of many structures [2], including the Chiasso Shed by Maillart [10] (sometimes known as Magazzini Generali), which is shown in Figure 10. The truss has many quads in it which indicate the presence of mechanisms. It is therefore important to determine the stability of these quads as they appear in numerous other structures including the Beghini Truss [2] and Ripshorst pedestrian bridge by SBP. Here we will focus on Maillart's truss.

Figure 10: *Chiasso Shed by Maillart [10].*

The truss has no static indeterminacies so cannot be self-stressed. A funicular must be applied to calculate the loads. However, the addition of the funicular removes the mechanism from the structure, as discussed in Section 2.3.3. Therefore, we find the forces in the structure with the funicular. The mechanism can be found by inspection of each quad. Using the methods discussed above, we calculate the stability of the rotation of each quad. Each quad is unstable in this analysis. This method gives us a value of K_s which is negative. The only reason the truss works in practice is that each node has a rotational stiffness. If the contribution to the stiffness by the joints is greater than K_s then the structure is stable, as is the case here. The stiffness and stability of the truss is very sensitive to the geometry. This is discussed in more depth in a separate paper by the authors [13].

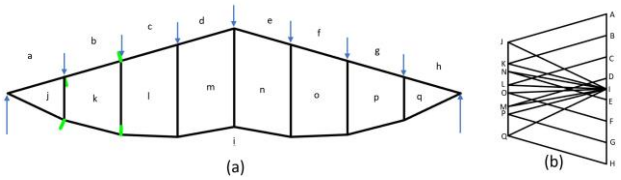

Figure 11: *Graphical analysis of Maillart's truss. (a) Form diagram with the mechanism investigated in green and the applied loads. (b) Force diagram.*

7. CONCLUSIONS

This paper presents a novel graphical method for determining the stability and stiffness of prestressable frameworks. Matrix based methods for these problems are well established but give many engineer little insight. This new method produces the same results but through a more engaging approach. This technique is extended to consider trusses which contain multiple mechanisms through the use of a reduced stress matrix which is also found graphically. Furthermore, vibrations of structures are considered with the aid of Rayleigh's principle. This technique allows the engineer to have greater control in the design of prestress stable structures and provides greater insight into the structural behaviour in comparison to previous matrix techniques. The ability to 'eye-ball' stability is also useful in the design process.

REFERENCES

[1] Konstantatou M. *et al*., n-dimensional graphic statics and structural transformations. Int. J. Solids Struct., 2018; 152-153; 272-293

[2] Beghini L. *et al*., Structural optimization using graphic statics. Struct. and Multidiscipl. Optim., 2014; 49.3; 351-366

[3] Guest S., The stiffness of prestressed frameworks: A unifying approach. Int. J. Solids Struct., 2006; 43.3-4; 842-854

[4] Connelly R. and Whiteley W., Second-order rigidity and prestress stability for tensegrity frameworks. SIAM Journal on Discrete Mathematics, 1996; 9 (3); 453-491

[5] Pellegrino S., Mechanics of Kinematically Indeterminate Structures, PhD Thesis, University of Cambridge, 1986

[6] McRobie, A., Maxwell and Rankine reciprocal diagrams via Minkowski sums for two-dimensional and three-dimensional trusses under load. Int. J. Space Struct., 2016; 31.2-4; 203-216

[7] McRobie A., *et al*., Mechanisms and states of self-stress of planar trusses using graphic statics, Part III: Applications and extensions, in IASS 2015. Future Visions

[8] McRobie A., *et al*., Graphic kinematics, visual virtual work and elastographics. Royal Society Open Science, 2017; 4.5

[9] Tarnai T., Problems Concerning Spherical Polyhedra and Structural Rigidity. Struct. Topology, 1980; 4; 61-66

[10] Zastavni. D., The Structural Design of Maillart's Chiasso Shed (1924): A Graphic Procedure. Struct. Eng. Int., 2008; 18; 247–252

[11] Maxwell, J.C., On Reciprocal Figures and Diagrams of Forces. Philos. Mag., 1864; 26; 250-261

[12] McRobie, A., Millar C., and Baker, W., Prestress Stability by Graphic Statics. Royal Society Open Science, submitted 31/10/2020

[13] McRobie, A., *et al*, Graphical Stability Analysis of Maillart's Roof at Chiasso. Struct. Eng. Int, submitted 21/08/2020